Article history: Received 26 December 2024, last revised 28 January 2025, accepted 3 February 2025



A NOVEL DEEP LEARNING APPROACHES FOR MULTI-CLASS HISTOPATHOLOGICAL SUB-IMAGE CLASSIFICATION USING PRIOR KNOWLEDGE

Riyam Ali Yassin¹, Morteza Valizadeh², and Alaa Hussein Abdulaal³

¹ Department of Electrical Engineering, Faculty of Electrical and Computer Engineering, Urmia University, West Azerbaijan, Iran. Email:Riyamaliyassin@gmail.com

² Department of Electrical Engineering, Faculty of Electrical and Computer Engineering, Urmia University, West Azerbaijan, Iran. Email:Mo.valizadeh@urmia.ac.ir

³ Department of Electrical Engineering, College of Engineering, Al-Iraqia University, Baghdad, Iraq. Email: Engineeralaahussein@gmail.com

https://doi.org/10.30572/2018/KJE/160340

ABSTRACT

Early diagnosis of breast cancer is critical for effective treatment and reducing mortality rates. Computer-aided diagnosis tools have become essential for identifying and diagnosing cancer in its initial stages. Convolutional neural networks (CNNs) have shown significant promise in medical image analysis, aiding in the detection of cancer cells and the classification of histopathological images through advanced data processing techniques. This study introduces a novel framework that combines transfer learning (TL) with an Incorporation of Prior Knowledge algorithm for multi-class classification of breast cancer using histopathological images. A new dataset comprising 3,600 sub-image histopathological images is presented, generated from the original Bach dataset. The study evaluates various pre-trained deep neural networks, including Inception V3, VGG19, GoogleNet, ResNet 101, and NASNet. Notably, the integration of prior knowledge and the focus on sub-image classification rather than whole images significantly enhanced cancer classification accuracy. The proposed method, leveraging the NASNet architecture, achieved a remarkable classification accuracy of 98.61%. Additionally, this study advances beyond conventional classification tasks by investigating tumor localization within breast cancer, utilizing sub-image analysis to improve diagnostic precision and support effective clinical decision-making. This innovative approach enhances



726

classification performance and contributes to more accurate tumor localization, thereby significantly improving diagnostic capabilities in breast cancer detection.

KEYWORDS

Breast Cancer, Histopathological, Computer Assisted Diagnosis, Deep Learning.

1. INTRODUCTION

Breast cancer (BC) is the most prevalent disease and cause of female mortalities in the universe. According to the International Agency for Research in Cancer, nearly 9.2 new female malignancies, 2.29 million of them, were cases of breast cancer (Ferlay et al., 2020). Breast cancer contributed to 15.5% of 4.4 million female malignancy-related deaths.

Early detection of cancer is delayed in most cases despite preventive processes such as imaging and mammography for screening, and it ends with a high fatality rate. According to the World Health Organization (WHO), 2.3 million females developed such a disease in 2020, and approximately 30% of them will not survive (Bergerot et al., 2022), (Wilkinson et al., 2021). Breast cancer is a complex etiological disease and one that is heterogeneous in consideration of acquired and genetic factors. Heterogeneity involves persons and malignancies, therefore introducing a range of prognosis and therapy (Ellsworth et al., 2017). In addition to gender (female) and age (over 40), other risk factors include being overweight, eating an imbalanced diet, abusing alcohol, and smoking (Dong et al., 2020), (Momenimovahed et al., 2019). BC is often caused by epithelial abnormalities (carcinoma), consisting of lesions that differ in microscopic characteristics and biological function. Breast cancer can be categorized into three grades: invasive forms (where tumor cells migrate to the breast stroma), metastatic carcinomas (where the tumor spreads to other locations), and noninvasive forms (in situ), in which tumor cells are confined to ducts or lobules. Non-invasive cancers may have lobular or ductal characteristics. The most prevalent kind of non-invasive cancer is called DCIS, and it is often linked to recidivism and the emergence of invasive ductal carcinoma, the invasive form of the disease. Infiltrating ductal carcinoma, another name for invasive ductal carcinoma, is the most frequent kind of breast cancer (Place et al., 2011).

Improving the patient's quality of life and overall chances of survival requires early diagnosis (Rock et al., 2022). Breast tissue biopsy images must be examined histologically to diagnose breast cancer. The four kinds of breast tissues include benign lesions, invasive carcinomas, in situ carcinomas, and normal breast tissues. Normal breast parenchyma tissue forms benign lesions, which have no connection to the development of malignant carcinogenesis. There are two forms of malignant breast cancer: invasive carcinomas and in situ carcinomas. Malignant cells are restricted in the mammary ductal-lobular system in the in-situ tissue, but they proliferate outside of the structure in invasive tissue. Pathologists use biopsy images stained with hematoxylin and eosin (H&E) to categorize and stage the tissue (Elston et al., 1991). Image scaling, rotation, and translation processes are needed throughout the study. This procedure requires highly skilled physicians and significant time and effort. Only 75% of pathologists'

diagnoses are accurate on average because of the complexity and diversity of histopathological images (Elmore et al., 2015).

Machine learning (ML) has made significant progress in recent years (Ruqaya Alaa et al., 2024). The potential of this topic has also developed for a wide variety of applications, including image recognition, medical diagnostics, defect identification, and building health assessments. The development of learning techniques that enable computer methods to carry out particular tasks based only on learned patterns, as well as an increase in the power of computers that supports these models' analytical capabilities, are just two of the many factors that have contributed to these new developments in ML (Perez et al., 2020).

Many machine-learning methods have been developed during the last ten years to classify breast cancer based on histopathology images (Juppet et al., 2021). Traditionally, early researchers used private datasets with small sample sizes to evaluate their methods and used standard machine-learning algorithms (George et al., 2014). Consequently, these techniques fall short of what clinical practice requires. CNNs have recently been widely used for BC classification (Dif et al., 2021). Techniques based on conventional networks, such as ResNet and Dense Net, have been proposed that have shown outstanding outcomes. However, in some earlier models, the raw image is often divided into patches to facilitate further analysis using convolutional neural networks (CNNs) (Mohammed et al., 2022). These patches retain the same labels as the original image extracted (Abdulaal et al., 2024a). This approach may lead to the CNN being trained on inaccurately labeled patches, which might have impacted the model's performance since benign problems can appear in malignant samples. Furthermore, accurate classification results are obtained by using sophisticated CNN models, which affect processing speed.

Medical images are an essential component of every patient's digital health dossier. Individual radiologists are restricted by time constraints, professional shortcomings, or a lack of expertise in producing such images. A radiologist's education takes decades and substantial financial resources. Furthermore, teleradiology is frequently employed in medical care to outsource radiological interpretations to countries with fewer economic resources. Teleradiology allows medical images such as X-rays, CT scans, and MRIs to be transmitted electronically to remote locations for analysis and diagnosis by radiologists. A delayed or incorrect analysis might harm the patient. As a result, autonomous, effective ML methods would be preferable for medical imaging (MI) investigations.

There are several types of imaging, and their use is becoming more common. Images from dermoscopy, ultrasound, X-rays, retinal scans, computed tomography (CT), positron emission

tomography (PET), and magnetic resonance imaging (MRI) are all instances of MI. Fig. 1 depicts several examples of MIs. Various imaging modalities, such as CT and MRI, can scan multiple organs within the body. In contrast, other imaging techniques, such as retinal and dermoscopy images, are specific to particular organs (Yousef et al., 2022).

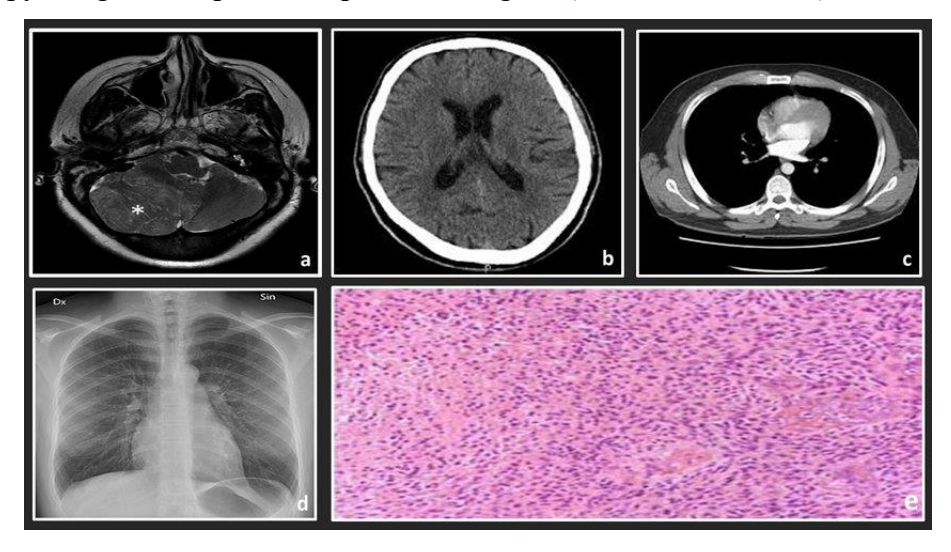


Fig. 1. shows different types of medical imaging, including (a) an MRI of the left side of the brain, (b) an axial CT brain scan, (c) an axial CT lung scan, (d) a chest X-ray, and (e) a histology slide showing high-grade glioma (Elazab et al., 2020)

This paper presents a novel approach that combines transfer learning (TL) with an Incorporation of Prior Knowledge algorithm for classifying breast cancer into four distinctive categories using histological images. This study will strive towards developing an algorithm that leverages transfer learning in pre-trained big datasets and then employs them in a new problem. This is a big step in that the model can gain an edge through information and trends gained in the pre-trained model, and accuracy and efficiency in classification can be increased. Besides, the "Incorporation of a Prior Knowledge" algorithm integrates preceding information. By combining TL with the incorporation of a prior knowledge algorithm, the proposed technology aims to classify BC into four types precisely. Hopefully, such a technique could promote awareness and diagnoses of BC through its histology images in a personalized therapy schedule and, in the long run, a better patient prognosis. Several deep neural networks with pre-training were considered for testing for effectiveness in the proposed techniques. Integration of prior knowledge and consideration for the classification of one single sub-image and not whole images effectively lowered the accuracy of cancer classification.

2. RELATED WORK

Several researchers have conducted studies on BC classification using CNNs for many years. (Zhu et al., 2019) suggested a hybrid strategy that included building many compact CNNs. A squeeze-excitation pruning block and local-global branches are all included in this approach.

These modules offered string representation and channel redundancy reduction. Experiments were carried out using the BreaKHis and BACH datasets. The multi-model assembly approach achieves results comparable to those of cutting-edge models. (Toğaçar et al., 2020) provide a residual architecture (BreastNet) with attention modules for classification. Attention modules aid in the identification of significant regions in the processed histopathology images. The hypercolumn method is used to get better results. BreastNet has an accuracy of 98.80%. E.M. (Nejad et al., 2017) investigated the importance of critical features in categorization and developed a unique single-layer CNN. This model extracts vital features from the images of the BreaKHis dataset, and their classification resulted in an accuracy of 77.5%. Using statistical and structural data included in the pathological images, (Nahid et al., 2018) classified them into two categories. The authors suggest a hybrid LSTM and CNN model. Conversely, the ultimate choice is made using SVM and SoftMax with 91.00% accuracy. Recurrent neural networks and CNN are used in the self-learning histopathological image processing system suggested by (Yan et al., 2019). His dataset is utilized in all experiments, and the images are classified into four groups with an accuracy of 91.3%. A DCNN with backpropagation, ensemble learning, and rectified linear unit (ReLU) activation functions is employed for intra-class classification (Adeshina et al., 2018). The study utilizes the BreaKHis dataset, achieving an accuracy of 91.5% across eight different classes. (Xie et al., 2019) carried out binary and multi-class classifications. InceptionResNetV2, in their work, extracted the input data's characteristics. A unique autoencoder was employed to translate those features into low-dimensional space, producing improved classification results. A model of inception-recurrent residual CNN was presented by (Alom et al., 2019) based on the promising outcomes of DCNN in previous studies. Transfers are usually helpful when the data size is small. (Khan et al., 2019) created a new technique for extracting features from pre-trained models like VGGNet, GoogleNet, and ResNet to accomplish binary classification. The suggested framework has an accuracy of 97.525%. In another study, (Aloyayri et al., 2020) implemented the binary classification challenge using the shuffleNet, InceptionV3, and ResNet18 architectures. These pre-trained architectures are trained using ImageNet. The last layers of the models are adjusted and trained using the BreaKHis dataset. The authors attained the maximum accuracy of 98.73%. (Ahmad et al., 2019) applied TL to ResNet, GoogleNet, and AlexNet, where 20 tests and 240 training images, divided into four groups, were employed. The ResNet approach attained the most remarkable accuracy of 85%. A transfer learning-based method was developed by (Mani et al., 2023) to classify BC images into four categories. That analysis made use of the BACH 2018 dataset. Two models, including ResNet50 and InceptionV3, were trained using the patches

obtained from those images. Both models were pre-trained using ImageNet. Accuracy of 97.50% was the highest level reported. (Murtaza et al., 2019) created a precise model for the classification of BC using TL. The model's final layer is tailored to perform binary classification using the AlexNet architecture. The extracted characteristics are then classified into two groups using six different machine learning methods, and an accuracy of 81.25% was reported on test data. (Ferreira et al., 2018) used a DNN with TL to categorize breast cancer. The authors used the ICIAR 2018 dataset to conduct the tests using a modified Inception ResNet V2 model. Its accuracy was 76%. The convolutional block attention module was proposed to detect metastases of BC automatically (Liang et al., 2019). A DL-based ensemble solution was proposed for the automatic binary categorization of histopathology images, yielding an accuracy of 97.6% on the PCam dataset. Feature extraction was performed via ensembles of the three architectures: MobileNet, DenseNet, and VGG19. It was evaluated by employing four publicly accessible datasets. On the BreaKHis dataset, the highest accuracy (98.13%) was reported by (Hameed et al., 2020). The BreaKHis and CMTHis datasets were classified by (Kumar et al., 2020) using VGGNet-16, which was trained on the ImageNet dataset. They attained an accuracy of 97% and 93% on those datasets.

(Balasubramanian et al., 2024) developed small CNNs to classify breast cancer based on histology samples. The authors used a design based on hybrid CNN, which combines local and global branches of the CNN model. The authors combined traits from these two branches to obtain vital attributes and employ local voting. Additionally, they improved classification results by ignoring undesirable channels or characteristics and using the suggested squeeze-excitation-pruning technique. By removing global and geographical information from areas of interest, (Ukwuoma et al., 2022) classified breast cancer histopathology images using a mixture of CNNs. The pre-trained CNNs employed by (Aljuaid et al., 2022) were ResNet18, ShuffleNet, and Inception-V3. On their BreaKHis dataset, the authors used transfer learning at different magnifications. Using data augmentation methods, including flips, rotations, and translations, they increased classification performance.

(Abdulaal et al., 2024a) proposed a self-learning DNN for the categorization of histological images of BC in recent research. They used TL and examined a great deal of pre-trained DNNs. To improve the accuracy of cancer classification, their work focuses on using a self-learning technique to categorize sub-images rather than the whole image. Nevertheless, a challenge arises when the classifier has to be trained using noisy labels since the true label of the sub-images is unknown. To avoid this, incorrect labels are gradually corrected using a hierarchical self-learning process based on prior information about the flaws in the original labels. The

suggested self-learning method uses the Inception-V3Net for four label correction rounds, resulting in an accuracy of 99.1%. Overall, using self-learning DNN to classify histological images of BC enhances precision and tailored therapy and improves efficiency, accuracy, and interpretability.

The current approaches, which required more time and processing power due to the complex structure's design, could only translate clinical images into a feature vector using several CNN architectures.

3. METHODOLOGY

This section highlights the significant contributions and strategies used for the multiclass classification of BC using histological images. Correctly classifying BC is crucial for an accurate diagnosis and appropriate treatment.

3.1. Multi-Class classification

Rapid advancements in deep learning algorithms and machine learning have recently posed new challenges for diagnosing breast histopathology images automatically. Multiclass classification, in terms of diagnosing histopathological images into various cancer subtypes or stages, has gained significant attention for it has important information for personalized therapy and prognosis.

The classification of breast histopathology images is particularly challenging due to its complex cellular structure and intrinsic tissue heterogeneity in form and arrangement. Variability in staining processes in histopathological images, in terms of degrees of magnification, and tissue preparation processes renders extraction of uniform discriminative features challenging. In addition, types of breast cancers vary in aggressiveness, and intratumorally heterogeneity creates additional difficulty in that regions in a single tumor can have specific histological features.

Therefore, to overcome these issues, many studies have examined several techniques and improvements developed in the multi-classification of breast histopathology images. A convolutional neural network is a deep neural network with state-of-the-art performance in image classification algorithms through its capability to learn hierarchical representations from raw picture information (Sivalingan, 2024).

Transfer Learning, which utilizes pre-trained networks over large datasets of images, has been utilized to extract important features and enhance accuracy in classification, predominantly when training information is not considerable.

The improvements in multiclass classification of breast histopathology images have exhibited tremendous potential for enhancing accuracy, velocity, and uniformity in BC diagnostics.

Pathologists can utilize automated sorters to make fewer mistakes in evaluations and even to provide additional care for a patient. In addition, such techniques can allow the processing of high volumes of histopathologic information to gain information about several dimensions of BC, such as the discovery of new biomarkers for a variety of types of disease

This study will investigate and contribute to the multiclass classification of histopathology breast images. It will strive to enhance accuracy and efficiency in the computerized classification of BC through state-of-the-art approaches to create personalized therapies with augmented patient care. Proper and efficient classification of BC through histopathology images is imperative for correct therapy planning and proper diagnosis. The development of DL algorithms in recent years seems to make such a classification computerized a reality.

Many studies have been performed to develop an efficient architecture for a CNN for classification in cases of BC. Several studies have analyzed and determined whether and to what extent DL can classify BC through histopathology images in several domains and regions. Due to this, several types of different architectures have been proposed and compared in detail for application in cases of classification of BC. Fig. 2 shows operations in such a mechanism.

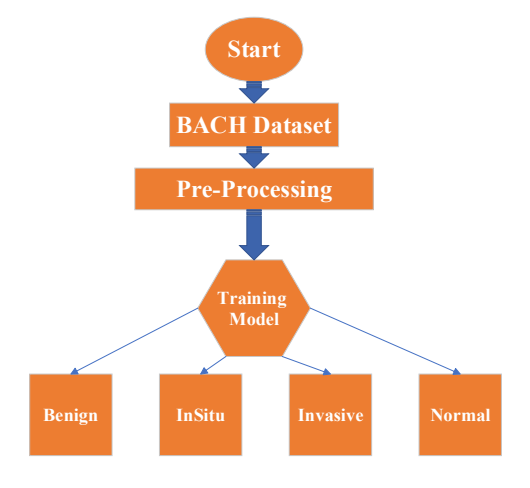


Fig. 2. Framework of the proposed multi-class classification

By comparing a range of several architectures of CNN, one can utilize the best model for classifying breast histopathology images into numerous subtypes and phases (Abdulaal et al., 2024d). Comparison and evaluation include comparing accuracy in classification, sensitivity, and specificity and testing for robustness with proper use of the BACH database (Araújo et al., 2017).

3.2. Dataset Description

The BC Histology Challenge 2018 (BACH) constructed the BACH dataset for histopathologic examination to classify carcinoma of the breast. It is utilized for testing and developing computer algorithms for classifying BC (Araújo et al., 2017).

The histopathologic slides in the dataset in BACH cover carcinoma, benign lesions, and carcinoma and normal epithelia in samples of breast tissue and with accompanying ground truth labels in the form of pixel-wise segmentation masks, such that fine-grained analysis and evaluation can be conducted. Trained pathologists accurately chose and labeled the dataset to allow for correct and reliable marking.

The photos in it have been captured under heterogeneous protocols regarding factors such as magnifications, representing diversity in observations in real-life practice.

The distribution of images in the BACH data concerning carcinoma types is shown in Fig. 3.

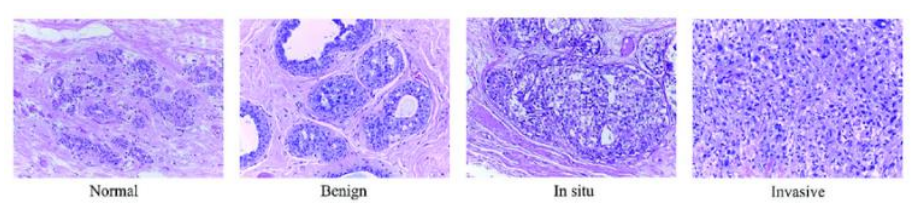


Fig. 3. BACH data set with four classes (Dong et al., 2020)

3.3. Data pre-processing

The Images of the BACH dataset required size normalization to ensure compatibility with the various networks used in this study. Data cropping and rescaling techniques align the image sizes with pre-trained deep neural networks. Specifically, several networks with distinct input image size requirements are utilized. For instance, ResNet 101 operates on 224 x 224 images, Inception-V3Net requires 299 x 299 images, VGG19 operates on 224 x 224 images, Google Net uses 224 x 224 images, and NASNet requires 331 x 331 images. Compatibility with the specific network architectures used in this study is ensured by resizing the input images accordingly. Data augmentation involves enriching the existing dataset by incorporating supplementary relevant information. The specific transformations applied in this study on Histopathological images included rotation, scaling, and flipping.

3.4. Proposed model

This study investigates the effectiveness of incorporating prior knowledge by training pretrained CNN models on the BACH dataset for tumor localization and classification. Specifically, NASNet yielded the most outstanding results among several pre-trained CNNs. Furthermore, we propose a novel approach for identifying tumor locations within sub-images using the trained CNN.

The BACH dataset consists of histology images related to BC, encompassing four classes: normal tissue, benign tumor, carcinoma in situ, and invasive carcinoma. To leverage prior knowledge, NASNet is a state-of-the-art pre-trained CNN architecture known for superior performance on image classification tasks. The benefit from the feature extraction efficiency of

NASNet images could be contained through pre-trained weights, which may lead to faster convergence and potentially result in better performance.

Transfer learning was used to modify NASNet for the BACH dataset. Fine-tuning the pretrained weights on this dataset enabled CNN architecture to learn tumor-specific features and adapt to histopathological characteristics, making it more accurate in identifying tumor regions. Apart from the tumor classification, a new technique for locating tumors within sub-images has developed. The trained NASNet model was applied to sub-images extracted from a histology image so that we could examine activation maps (or feature maps) produced by CNN. These maps showed areas with high activations corresponding to potential regions of cancerous growth. Therefore, this method can be valuable for detecting tumor cells and suspicious parts in images.

A NASNet has been created for BC multi-classification by investigating these histopathological images, as illustrated in Fig. 4.

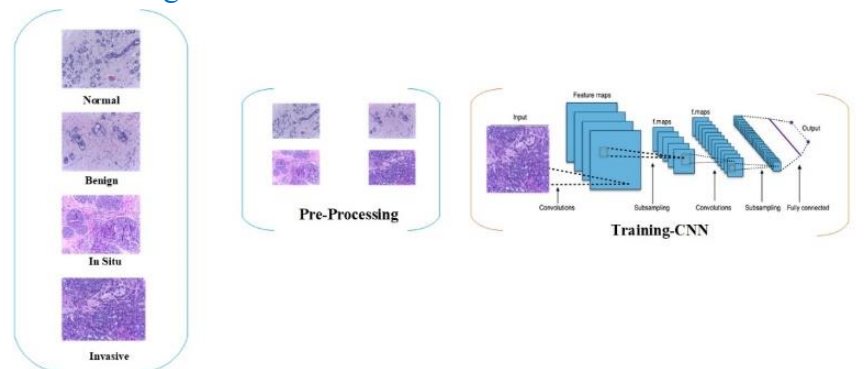


Fig. 4. NASNet CNN.

In the first place, every image from the BACH dataset was divided into nine parts to capture more localized information, as indicated in Fig. 5.

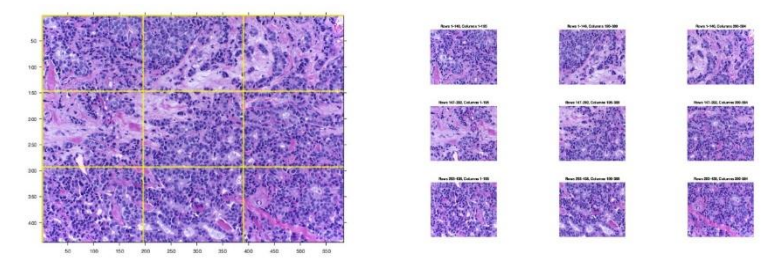


Fig. 5. Pre-processing operation.

Then, benign sub-images are tested and classified into normal and benign. This classification process is a crucial part of the testing procedure.

After collecting the benign sub-images, they are subjected to rigorous tests using the NASNet model. This model uses image recognition technology and capitalizes on its ability to accurately detect and label these images based on their features.

During this testing stage, benign sub-images will be put in the classifying model, which will be

used to observe them for visual attributes and patterns. As shown in Fig. 6 below, based on this analysis, the model assigns each sub-image to either the normal or benign classes.

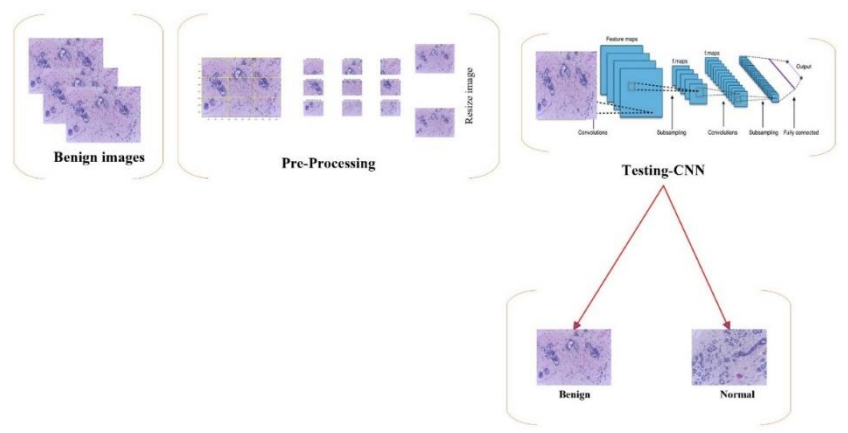


Fig. 6. Benign sub-images Testing with NASNet.

Various applications and studies depend on classifying the sub-images as benign or normal. Valuable information is provided that distinguishes normal cases from those with benign abnormalities.

After classifying the sub-images, some regions were labeled as benign. These areas were potential sites for tumors within the original image. Tumors can be seen in histopathological images by recognizing and determining their location. Then, these in-situ sub-images will undergo thorough testing using the NASNet model.

While still in the testing stage, in-situ sub-images would be inserted into the NASNet model, which should be analyzed based on their features and patterns. Based on this analysis, each sub-image is assigned to one of three classes according to Fig. 7: Normal, Benign, or In Situ.

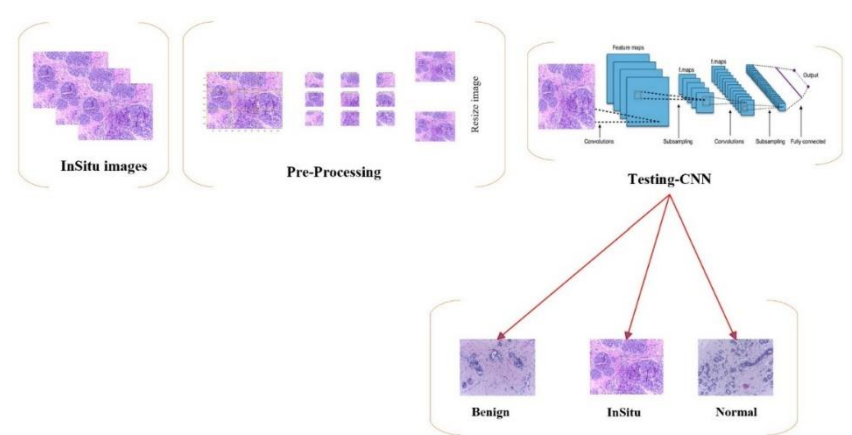


Fig. 7. Testing of In-situ sub-images with NASNet.

In this context, it is essential to differentiate these in-situ sub-images into separate classes for further examination and decision-making purposes. This will recognize normal, benign, and in situ cases.

The testing process, therefore, aims to provide accurate and reliable results that will facilitate professionals' and researchers' better understanding of the nature and classification of in-situ

sub-images using NASNet. These revelations can then assist in several ways, including diagnosis, treatment schedules, or future research developments within the field.

Invasive sub-images are tested to separate them into four unique classes: normal, benign, in situ, and invasive.

Once collected, advanced classification techniques will be applied to the invasive sub-images. Such algorithms utilize deep learning, and through it, proper analysis and classification will be guaranteed with certain attributions and qualifications in such an image. The testing involves considering such a visual feature and a sequence of an invasive sub-image with a classification model. The sub-images analyzed will fall under one of four groups: normal, benign, in situ, and invasive Fig. 8.

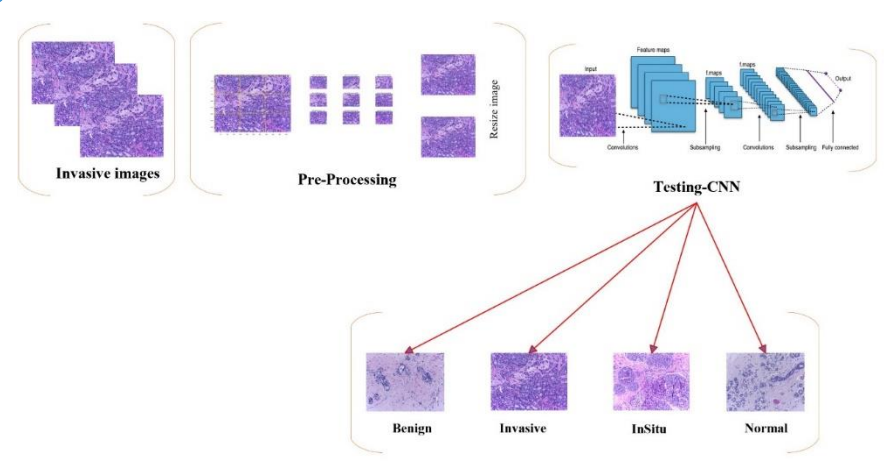


Fig. 8. Invasive sub-images Testing with NASNet

Classifying the invasive sub-images into these four classes is highly significant in various spheres. It enables separation between normal cases, benign abnormalities, in-situ conditions, and invasive malignancies, providing crucial details for diagnostics, treatment planning, and further research analysis. The new dataset is presented in Table 1.

	Table 1. New Dataset									
Class	BACH	Sub-Ima	New-N	New-B	New-InS	New-Inv				
N	100	900	900	X	X	X				
В	100	900	302	598	X	X				
InS	100	900	183	116	601	X				
Inv	100	900	111	83	209	497				
Total	400	3600	3600							

Upon evaluating a pre-trained deep neural network (DNN), a NASNet DNN 2 model was developed to classify a new dataset, as outlined in Table 1. The dataset comprised 3600 images, and a 5-fold cross-validation methodology was employed to ensure rigorous assessment.

After classifying the patches, the next step involves collecting sub-images to reconstruct the original image. These sub-images are extracted based on the patches from the previous classification step. The patches classified as potentially malignant (either in Situ or Invasive) are of particular interest and are carefully examined.

The sub-images are reconstructed by gathering the classified patches per their places in the original image. The complete image is reconstructed by combining these patches to allow for a thorough analysis of the whole image.

Finally, its overall classification is determined once the original image has been reconstructed. This classification can include malignant (in situ or Invasive), benign, or normal. This decision is based on whether malignant parts in the in situ and Invasive regions exist in the reconstructed image. The image is considered malignant if even one patch is classified as cancerous (in situ or Invasive), as shown in Fig. 9. Fig. 10 shows a flowchart for incorporating a prior knowledge technique.

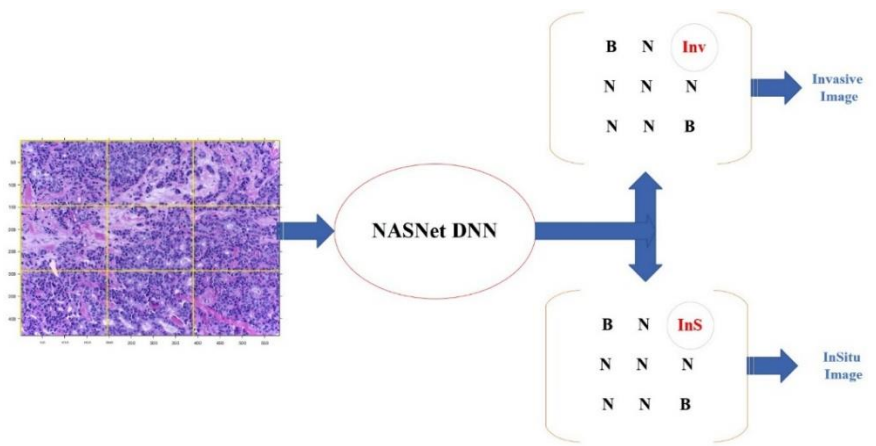


Fig. 9. Reconstruction and Decision Based on Patch Classification for Malignant Regions

3.5. Cross-Validation

The crucial cross-validation method evaluates ML models' performance and generalization capabilities. In this work, 5-fold cross-validation is utilized to test the performance of multiclass classification models. The four principal classes in the histopathological images in the BACH-2018 dataset include in situ, Invasive, benign, and normal.

The training and testing sets divide the dataset, with 80 percent of samples and 20 percent of samples, respectively. The models' performance is evaluated via 5-fold cross-validation. In 5-fold cross-validation, training sets are partitioned into five folds, with an even number of samples for each fold. The model is trained five times, and during evaluation, one of the folds is taken as a testing set, and others become training subjects.

Through 5-fold cross-validation and evaluation with such performance measures, such a mechanism provides important information regarding model performance. Such a mechanism reduces overfit and yields performance measures for model generalizability.

The multi-class classification model with a CNN model can be represented in Fig. 11.

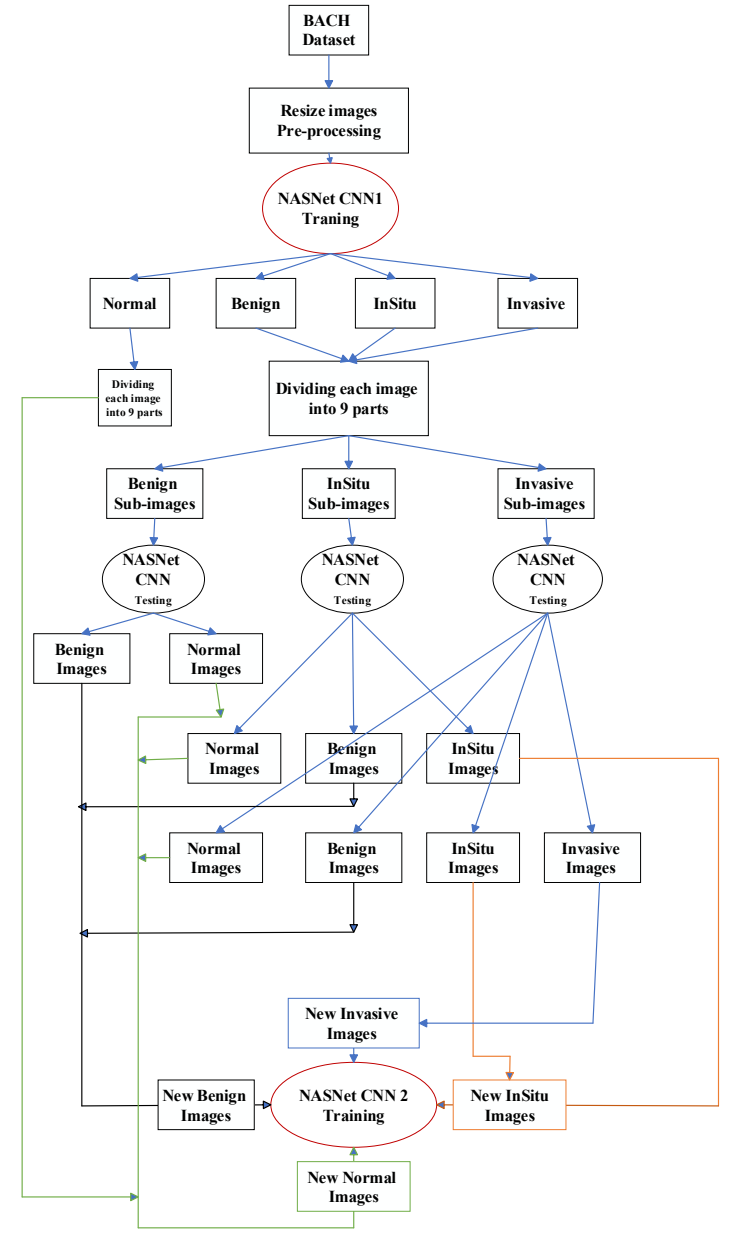


Fig. 10. Framework for incorporating prior knowledge of DNNs.

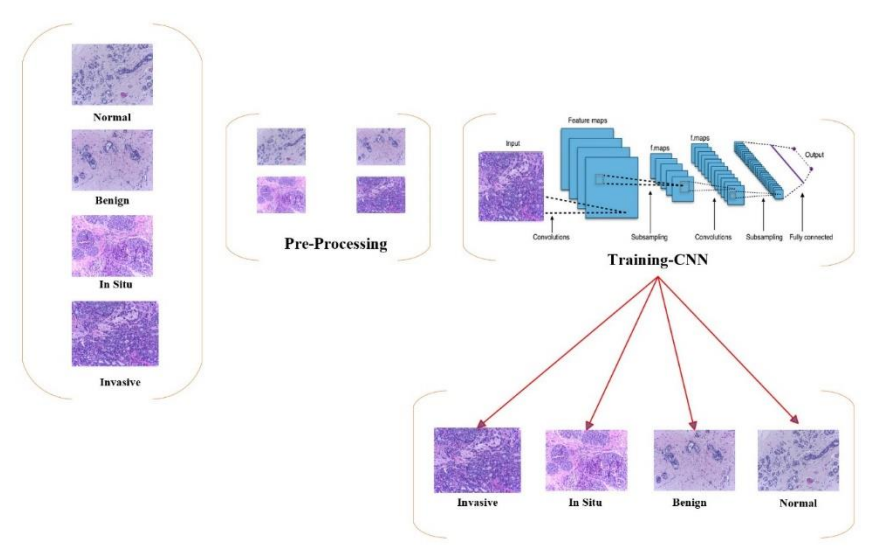


Fig. 11. CNN for multi-class classification

3.6. Pre-trained Deep Neural Networks

Histopathological image analysis is an integral part of medical diagnostics, for which rapid and accurate classification of tissue samples is critical for proper therapy planning, prognosis, and diagnosis. Histopathology image classification has been enormously facilitated through DL with pre-trained DNNs, which have attained high performance in terms of high accuracy values. Neural networks have been trained over large datasets, such as ImageNet, to identify visual patterns. These networks obtain hierarchical information from an image, through which complex representations and patterns can be extracted. The application of pre-trained DNNs for histopathology image classification has a range of useful factors, including less training duration and effective generalization performance over unknown information. There have been a range of pre-trained DNN architectures for histopathology image classification, which have widespread use.

Five architecture-based pre-trained deep neural network classifiers (DNNs) (Abdulaal et al., 2024b) have been used in the current work. Inception V3, GoogleNet, VGG19, ResNet-101, and NASNet have been considered in work with these classifiers. These DNNs have a high potential for autonomously extracting meaningful information from imaging information.

3.6.1. VGG

The Visual Geometry Group Net (VGG) is a model developed at Oxford Robotics Institute for a model for a CNN. VGGNet performed admirably at ImageNet, with approximately one million examples of 1000 categories, having trained and produced an astonishing 138 million parameters to tune. VGG19 won first in 2014's Classification and Localization Challenge (Zakaria et al., 2024).

The VGG family networks include VGG11, VGG13, VGG16, and VGG19, TL (transfer learning) networks. VGG19 specifically consists of five individual blocks. Two blocks from the first two consist of a convolution and one of a pooling block. The third and fourth blocks comprise four convolutional layers and one pooling layer each. The final building element consists of four convolutional layers. Additionally, three additional smaller filters are utilized.

3.6.2. ResNet101

ResNet, an acronym for residual network, was constructed from several layers that were joined in a certain way and instructed to do different tasks (Shafiq et al., 2022). The output from the preceding layer is used directly by the residual connection (9 of the 33 levels). The remaining connections serve as the operands for summation operations. The four subsequent layers—a convolutional layer with a filter size of 1 x 1 and a stride of 1 followed by a series of normalization layers—use the output of the previous block as their input.

3.6.3. Inception-V3Net

The Inception-V1 has been upgraded to the Inception-V3. The Inception-V3 model took several actions to boost the model flexibility and enhance the network efficiency (Bhatt et al., 2021). Compared to the models Inception-V1 and V2, it has a deeper network. A deep CNN that was directly trained on a low-end computer is the Inception-V3 model. Training of deep models may take many days. By keeping the last layer of the model for new categories, TL avoids this difficulty. The pre-trained version of the Inception-V3 model is obtained by retaining the weights of all layers except the weights of classification layers, whose weights are adjusted using the task-specific data set.

3.6.4. GoogleNet

Google Net model contains twenty-two levels of network structure. The model includes the Google team's recommended inception structure and the convolution, pooling, and fully connected layers. Various visual features may be produced using convolutional kernels in the inception structure with different scales (Abdulaal et al., 2024c).

The GoogleNet model's multi-layer CNN structure and inception structure may be responsible for its exceptional performance in image recognition. Nine inception modules make up the initial architecture of the GoogleNet model. The inception v1 has a 3x3 pooling layer and three convolutional layers with 1x1, 3x3, and 5x5 kernels. This structure processes images in parallel and then stacks them together to widen the network and its capacity. More convolutional kernel parameters will follow suit with more channels in an input image. It is, therefore, critical to downsize to manage increased computational demand. One such mechanism includes 1x1 convolutional layers, which neither preserve height nor width in an image but can downsize channels in the count. Hierarchically employing 1x1 convolutional kernels preceding 3x3 and 5x5 kernels and following 3x3 max-pooling layers can downsize feature map depth (Alkhodari et al., 2021).

3.6.5. **NASNet**

NASNet-Mobile is trained with the ImageNet dataset. With an active feature, NASNet labeled images successfully. NASNet Mobile and NASNet Large are classes with most of the NASNet structure. In contrast, the NASNet Mobile network is optimized best for smaller data sets than NASNet Large. It seeks the best convolutions in relatively small sets of data. Higher performance in classification and less computational expense were achieved when utilized with convolutional cells. In NASNet, free parameters in terms of model complexity, computational expense, and desired performance are utilized in terms of both cells, blocks, and initial convolution filter numbers that such a search algorithm must discover. It searches alternative

structures and configurations in its search algorithm to receive the best values for such free parameters in terms of model complexity, computational expense, and desired performance (Vallabhajosyula et al., 2021).

3.7. Dataset Experimental Protocol

In this work, the model has been trained with a DNN model with an image-based model for learning. 5-fold cross-validation is performed using a BACH dataset to test performance in such a model. Optimization uses an Adam optimizer with an adaptive estimation of a moment with predefined parameter sets. The decay factor was 0.99, the batch size was 128, and the learning rate was 0.0001, and these have been utilized for enhancing training and convergence performance.

Evaluation metrics assess the performance of classifiers, including precision, sensitivity, classification accuracy, specificity, and F1 score. All these indications report on the performance of such a model and, therefore, for testing for suitability and efficiency in such an application.

3.8. Evaluation metrics

This paper utilizes a variety of evaluation factors in measuring classifier performance and efficiency. These factors shed light on classifier predictive performance and allow one to objectively make comparative efficiencies regarding a variety of classification concerns. The following section discusses evaluation factors and measures utilized (Abdulaal et al., 2024e). A confusion matrix is a useful evaluation tool that imparts immediate information regarding a classifier's performance, particularly for many classes. A confusion matrix represents actual instances for a class in a column and predicted instances for a class in a row. It is a square matrix. As Table 2 shows, a 4x4 structure of a confusion matrix for four-class classification is utilized.

Table 2. Confusion Matrix									
	Predicted Class								
	Normal Benign In Situ Invasive								
	Normal	TP	FN	FN	FN				
Actual	Benign	FN	TP	FN	FN				
	In Situ	FN	FN	TP	FN				
	Invasive FN FN FN TP								

Instances correctly classified as belonging to a particular class are known as True Positives (TP).

Samples that are mistakenly classified as not belonging to a particular class are known as false negatives (FN).

The classification accuracy (1) measures the total accuracy of the classifier's predictions. It is determined by dividing the correctly classified instances by the total number of samples in the dataset. A higher level of accuracy indicates better performance, with 100% accuracy indicating that all predictions are correct (Abdulwahhab et al., 2024).

$$Accuracy = \frac{(TP_A + TP_B + TP_C + TP_D)}{N} \tag{1}$$

Where:

TP_A, TP_B, TP_C, and TP_D are the true positives (correctly classified samples) for Normal, Benign, In Situ, and Invasive.

N is the total number of samples in the dataset.

Sensitivity (2), often called recall or true positive rate, quantifies the percentage of real positive events that the classifier accurately detects. It is determined as the proportion of true positive predictions to all positive examples. A greater sensitivity suggests better performance in capturing all positive examples, which gives insight into the classifier's capacity to recognize positive instances accurately.

Sensitivity (Class
$$X$$
) = $\frac{TP_X}{(TP_X + FN_X)}$ (2)

Where:

TP_X: True Positives for class X

FN_x: False Negatives for class X

Precision (3) is the percentage of all positive cases that the classifier correctly predicted out of all positive instances. It is measured as the proportion of true positive predictions to all expected positive samples. Precision, which measures how accurately the classifier labels occurrences of positivity, is beneficial when the cost of false positives is significant. Lower false-positive predictions are indicative of higher accuracy.

Precision (Class
$$X$$
) = $\frac{TP_X}{(TP_X + FP_X)}$ (3)

Where:

FP_X: False Positives for class X

The F1 score (4) is a composite statistic compromising sensitivity and accuracy. It provides a single metric to assess the classifier's effectiveness and is the harmonic mean of accuracy and sensitivity. The highest F1 score is 1, indicating perfect sensitivity and accuracy, while its lowest is 0. A higher F1 score indicates better coordination of sensitivity and accuracy.

$$F1score\left(Class\ X\right) = \frac{2*\left(Precision_X * Sensitivity_X\right)}{\left(Precision_X + Sensitivity_X\right)} \tag{4}$$

Where:

Precision X is the precision for class X.

Sensitivity X is the sensitivity (recall) for class X.

Another term for specificity (5) is the percentage of true negative cases detected by the classifier. It can be obtained by dividing the total number of actual negatives by the number of all samples classified as such. When what matters most is an accurate classification of negative samples, specificity is one way to find out. The greater specificity suggests better accuracy in the correct classification of negative cases.

Specificity (Class
$$X$$
) = $\frac{TN_X}{(TN_X + FP_X)}$ (5)

Where:

TN_X: True Negatives for class X

4. RESULTS

This section presents the outcomes of tests carried out on multiple classification tasks of breast cancer using histopathology images. Six DNNs trained with TL methods were used in these tests. This evaluation was based on the publicly available BACH dataset grouped into four classes.

The data set was divided into two parts for training and testing: a training set that accounted for 80% and a testing set composed of the remaining 20%. A five-fold cross-validation technique was used to ensure the models' performance was robustly assessed during these tests.

NASNet DNN 2 was also included in addition to the previous one to classify a new dataset comprising 3600 specially curated images aimed at multiclass classification. Consequently, this allowed an overall assessment of how well these models performed under multiclassification.

4.1. Performance of Pre-trained Deep Neural Networks

This section presents the classification outcome of six types of Deep Neural Network (DNN) classifiers: VGG19, ResNet101, GoogLe Net, Inception V3 Net, NASNet 1, and NASNet 2. These classifiers were tested on the BACH dataset, which consists of images related to BC. Table 3 provides results to evaluate and compare these DNNs' performance and visual presentations in Figs. 12, 13, and 14. Remarkably, however, NASNet shows the best performance among all evaluated metrics.

Table 3. Performance Metrics

No.	CNN	Class	Benign	InSitu	Invasive	Normal	Average
		Accuracy			96.25		_
		Precision	97	97	96	95	96.25
1	GoogleNet	Recall	94.17	97.98	97.96	95	96.28
	_	F1-Score	95.57	97.49	96.97	95	96.26
		Sensitivity	94.17	97.98	97.96	95	96.28
		Specificity	98.99	99	98.68	98.33	98.75
		Accuracy			94.5		
		Precision	95	95	93	95	94
2	Inception	Recall	95	95.96	94.9	92.23	94.52
	V3	F1-Score	96.86	97.53	95.59	95	96.25
		Sensitivity	95	95.48	93.94	93.6	94.5
		Specificity	98.33	98.34	97.68	98.32	98.17
		Accuracy			97.25		
		Precision	97	99	95	98	97.25
3	ResNet101	Recall	97.98	95.19	97.94	98	97.28
		F1-Score	97.49	97.06	96.45	98	97.25
		Sensitivity	97.98	95.19	97.94	98	97.28
		Specificity	99	99.66	98.35	99.33	99.09
		Accuracy			98.25		_
		Precision	99	100	98	96	98.25
		Recall	97.06	99.01	98	98.97	98.26
4	NasNet	F1-Score	98.02	99.5	98	97.46	98.25
		Sensitivity	97.06	99.01	98	98.97	98.26
		Specificity	99.66	100	99.33	98.68	99.42
		Accuracy			95.5		
		Precision	95	94	96	97	95.5
		Recall	94.06	95.92	96.97	95.1	95.51
5	VGG19	F1-Score	94.53	94.95	96.48	96.04	95.49
		Sensitivity	94.06	95.92	96.97	95.1	95.51
		Specificity	98.33	98.01	98.67	98.99	98.5
		Accuracy			98.61		
		Precision	97.49	98.15	98.59	99.46	98.42
6	NasNet2	Recall	98.61	98.64	96.84	99.20	98.32
		F1-Score	98.05	98.39	97.71	99.33	98.37
		Sensitivity	98.61	98.64	96.84	99.20	98.32
		Specificity	99.29	99.46	99.77	99.62	99.54

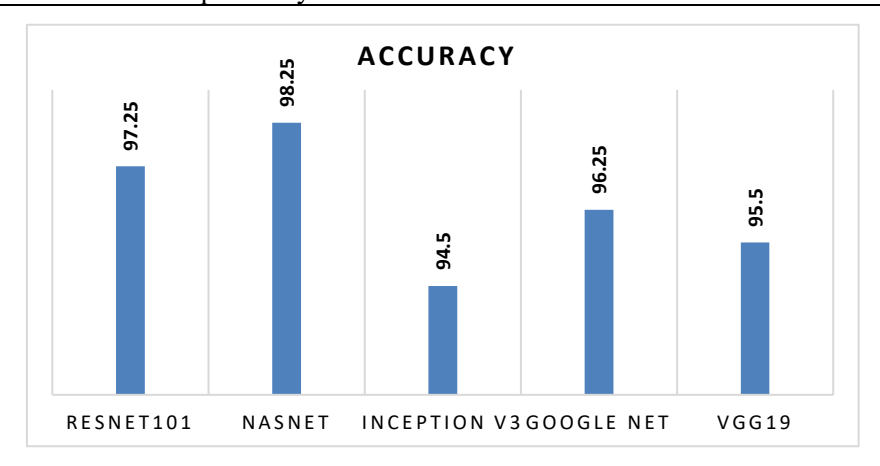


Fig. 12. Accuracy of different DNNs.

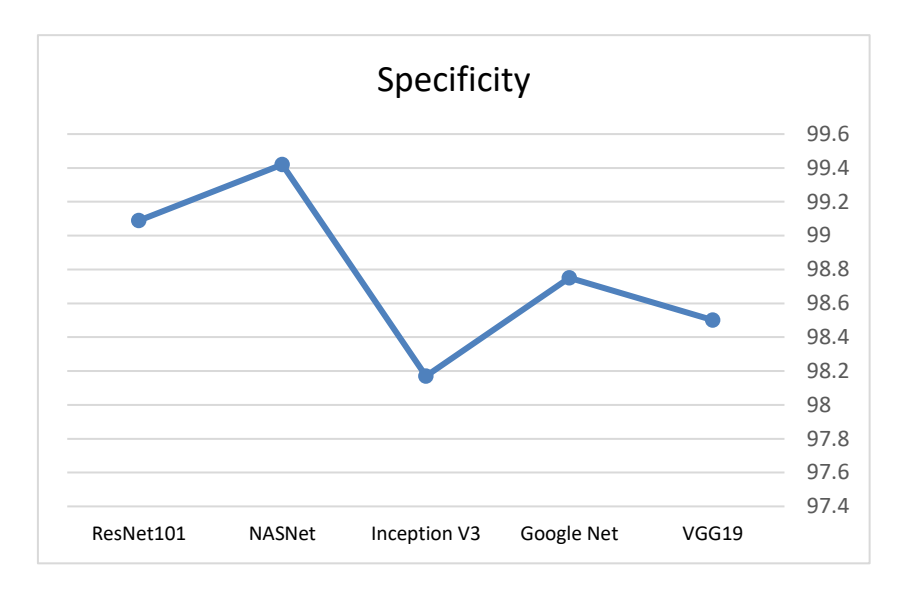


Fig. 13. Specificity of Five DNNs.

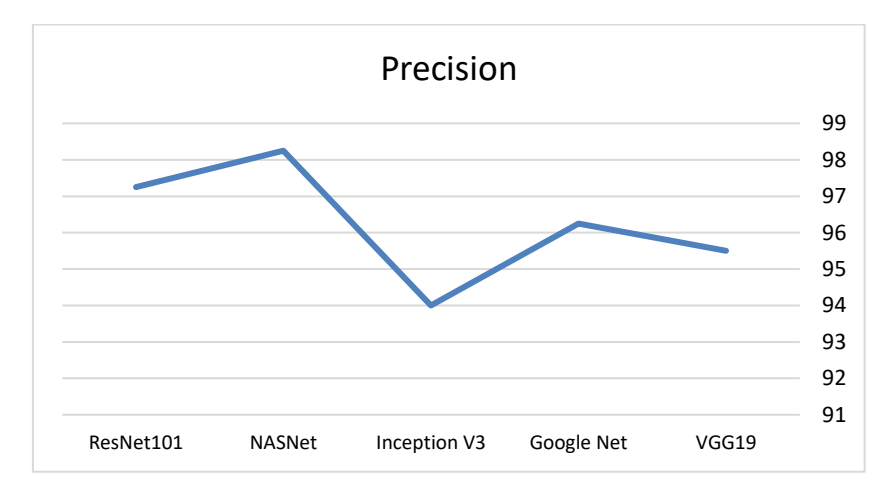


Fig. 14. Precision of Five DNNs.

4.2. Confusion Matrices

A confusion matrix is a tool that compares the actual and predicted classifications made by any classification model. It provides a detailed summary assessment of model performance.

Table 4 presents confusion matrices applied to several DNNs: VGG19, Inception-V3, ResNet101, Google Net, and NASNet. These matrices indicate their performance in terms of distribution among different categories of correct and wrong predictions.

In summary, the results indicate that NASNet has achieved an impressive accuracy rate of 98.61%. This underscores NASNet's success in delivering superior performance compared to other models. Fig. 15 showcases the accuracy metrics and the convergence loss for the best model, which in this case is NASNet.

	Table 4. Confusion Matrices								
No.	CNN	Class	Benign	InSitu	Invasive	Normal			
		Benign	97	1	1	4			
		InSitu	1	97	0	1			
1	GoogleNet	Invasive	1	1	96	0			
	C	Normal	1	1	3	95			
					400				
		Benign	95	1	3	1			
		InSitu	2	95	1	1			
_				_		_			

		InSitu	1	97	0	1
1	CanalaNat		1	1	96	0
1	GoogleNet	Invasive				-
		Normal	1	1	3	95
					00	
		Benign	95	1	3	1
		InSitu	2	95	1	1
2	Inception	Invasive	0	2	93	3
	V3	Normal	3	2	3	95
				4	00	
		Benign	97	0	2	0
		InSitu	2	99	2	1
3	ResNet101	Invasive	0	1	95	1
		Normal	1	0	1	98
				4	00	
		Benign	99	0	1	2
		InSitu	0	100	0	1
4	NasNet	Invasive	1	0	98	1
		Normal	0	0	1	96
				4	00	
		Benign	95	3	2	1
		InSitu	3	94	0	1
5	VGG19	Invasive	1	1	96	1
		Normal	1	2	2	97
				4	00	
		Benign	778	6	3	2
		InSitu	6	795	2	3
6	NasNet2	Invasive	8	5	490	3
		Normal	6	4	2	1487
			-		500	
-						

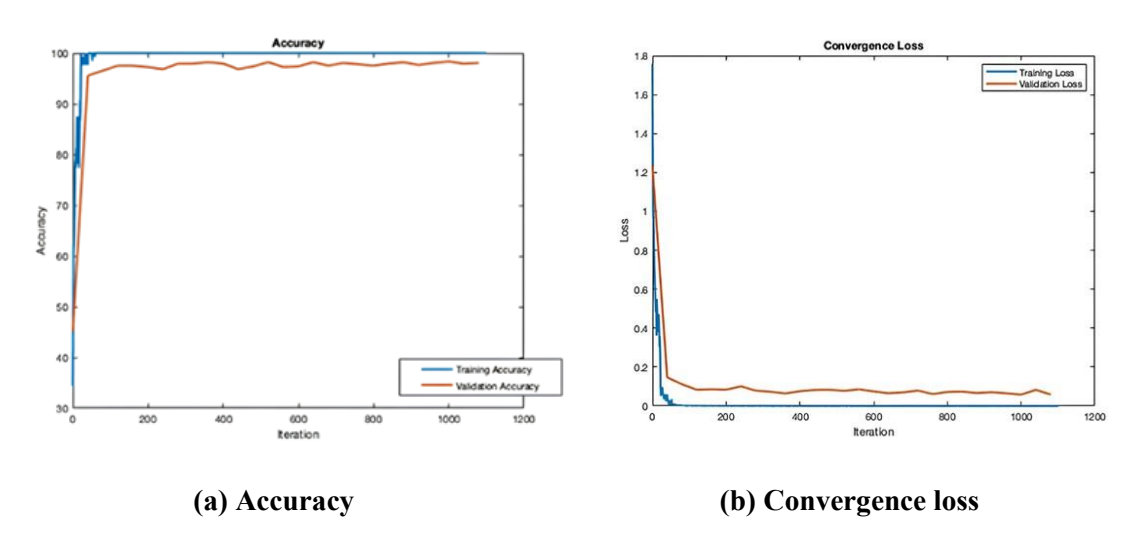


Fig. 15. Accuracy and Convergence loss curves

Table 5 summarizes the most relevant research efforts reviewed that have been carried out with the same database.

Years	Model	Class	Accuracy	Specificity	Sensitivity	Precision	F1 score
(Meng et al.,	ResNet	4	91%	91%	-	93%	-
2019)							
(Yao et al.,	Parallel	4	92%	92%	-	90%	-
2019)	CNN						
(Zhou et al.,	RaNet	4	97.75%	98.21%	-	97.93%	-
2022)							
(Balasubramani	Ensemble	4	98.43%	-	-	-	-
an et al., 2024)	Models						
(Sreelekshmi et	SwinCNN	4	93%	-	91.40%	93%	93%
al., 2024)							
2025	This Work	4	98 61%	99 54%	98 32%	98 42%	98 37%

Table 5. Comparison with other related works

5. CONCLUSION

This study significantly advances breast cancer (BC) classification by incorporating prior knowledge to enhance diagnostic accuracy. Through a comprehensive evaluation of various pre-trained deep learning models, this research has illuminated a novel approach to BC diagnosis using histopathological images. Introducing a new dataset, consisting of 3,600 sub-image histopathological images generated from the original BACH dataset, has provided a robust foundation for analysis.

By employing six pre-trained convolutional neural networks (CNNs) and utilizing an image-based methodology, the study effectively demonstrated the potential of Transfer Learning (TL) in adapting models for improved performance. Innovative techniques, such as data augmentation, were implemented to enhance the training dataset, ultimately leading to remarkable results. NASNet emerged as a standout performer, achieving an impressive mean classification accuracy of 98.61%.

Furthermore, this research ventured beyond traditional classification tasks to explore tumor localization within breast cancer, showcasing the efficacy of sub-image analysis. Leveraging the power of prior knowledge, the proposed methodology for accurately identifying tumor locations within sub-images and analyzing activation maps offers a promising avenue for improving diagnostic capabilities. This innovative approach enhances classification performance and contributes to better patient care and outcomes in breast cancer management, underscoring the importance of early diagnosis and accurate localization in the fight against this disease.

6. REFERENCES

Abdulaal, A. H., Dheyaa, N. H., Abdulwahhab, A. H., Yassin, R. A., Valizadeh, M., Albaker, B. M., & Mustaf, A. S. (2024b). Deep Learning-based Signal Identification in Wireless Communication Systems: a Comparative Analysis on 3G, LTE, and 5G Standards. Al-Iraqia

Journal for Scientific Engineering Research , 3(3), 60–70. https://doi.org/10.58564/IJSER.3.3.2024.224

Abdulaal, A. H., Valizadeh, M., AlBaker, B. M., Yassin, R. A., Amirani, M. C., & Shah, A. F. M. S. (2024c). Enhancing Breast Cancer Classification Using a Modified GoogLeNet Architecture with Attention Mechanism. Al-Iraqia Journal of Scientific Engineering Research, 3(1). https://doi.org/10.58564/ijser.3.1.2024.145

Abdulaal, A. H., Valizadeh, M., Amirani, M. C., & Shahen Shah, A. F. M. (2024a). A self-learning deep neural network for classification of breast histopathological images. Biomedical Signal Processing and Control, 87, 105418. https://doi.org/10.1016/j.bspc.2023.105418

Abdulaal, A. H., Valizadeh, M., Yassin, R. A., Albaker, B. M., Abdulwahhab, A. H., Amirani, M. C., & Shah, S. (2024d). Unsupervised Histopathological Sub-Image Analysis for Breast Cancer Diagnosis Using Variational Autoencoders, Clustering, and Supervised Learning. Journal of Engineering and Sustainable Development, 28(6), 729–744. https://doi.org/10.31272/jeasd.28.6.6

Abdulaal, A. H., Yassin, R. A., Valizadeh, M., Abdulwahhab, A. H., Jasim, A. M., Mohammed, A. J., Jabir, H. J., Albaker, B. M., Dheyaa, N. H., & Amirani, M. C. (2024e). Cutting-Edge CNN Approaches for Breast Histopathological Classification: The Impact of Spatial Attention Mechanisms. ShodhAI: Journal of Artificial Intelligence, 1(1). https://doi.org/10.29121/shodhai.v1.i1.2024.14

Abdulwahhab, A. H., A. H. Abdulaal, Assad, A. A. Mohammed, & M. Valizadeh. (2024). Detection of Epileptic Seizure Using EEG Signals Analysis Based on Deep Learning Techniques. Chaos, Solitons & Fractals/Chaos, Solitons and Fractals, 181, 114700–114700. https://doi.org/10.1016/j.chaos.2024.114700

Adeshina, S. A., Adedigba, A. P., Adeniyi, A. A., & Abiodun Musa Aibinu. (2018). Breast cancer histopathology image classification with deep convolutional neural networks. 2018 14th International Conference on Electronics Computer and Computation (ICECCO), 206–212. https://doi.org/10.1109/icecco.2018.8634690

Ahmad, H. F., Ghuffar, S., & Khurshid, K. (2019). Classification of breast cancer histology images using transfer learning. International Bhurban Conference on Applied Sciences and Technology. https://doi.org/10.1109/ibcast.2019.8667221

Aljuaid, H., Alturki, N., Alsubaie, N., Cavallaro, L., & Liotta, A. (2022). Computer-aided diagnosis for breast cancer classification using deep neural networks and transfer learning. Computer Methods and Programs in Biomedicine, 223, 106951. https://doi.org/10.1016/j.cmpb.2022.106951

Alkhodari, M., & Fraiwan, L. (2021). Convolutional and recurrent neural networks for the detection of valvular heart diseases in phonocardiogram recordings. Computer Methods and Programs in Biomedicine, 200, 105940. https://doi.org/10.1016/j.cmpb.2021.105940

Alom, M. Z., Yakopcic, C., Nasrin, Mst. S., Taha, T. M., & Asari, V. K. (2019). Breast cancer classification from histopathological images with inception recurrent residual convolutional neural network. Journal of Digital Imaging, 32(4), 605–617. https://doi.org/10.1007/s10278-019-00182-7

Aloyayri, A., & Krzyżak, A. (2020). Breast cancer classification from histopathological images using transfer learning and deep neural networks. Artificial Intelligence and Soft Computing, 19(Part I), 491–502. https://doi.org/10.1007/978-3-030-61401-0_45

Araújo, T., Aresta, G., Castro, E., Rouco, J., Aguiar, P., Eloy, C., Polónia, A., & Campilho, A. (2017). Classification of breast cancer histology images using convolutional neural networks. PLOS ONE, 12(6), e0177544. https://doi.org/10.1371/journal.pone.0177544

Balasubramanian, A. A., Awad, M., Singh, A., Breggia, A., Ahmad, B., Christman, R., Ryan, S. T., & Amal, S. (2024). Ensemble deep learning-based image classification for breast cancer subtype and invasiveness diagnosis from whole slide image histopathology. Cancers, 16(12), 2222. https://doi.org/10.3390/cancers16122222

Bergerot, C. D., Dizon, D. S., Ilbawi, A. M., & Anderson, B. O. (2022). Global breast cancer initiative: A platform to address the psycho-oncology of cancer in low- and middle-income countries for improving global breast cancer outcomes. Psycho-Oncology, 32(1), 6–9. https://doi.org/10.1002/pon.5969

Bhatt, D., Patel, C., Talsania, H., Patel, J., Vaghela, R., Pandya, S., Modi, K., & Ghayvat, H. (2021). CNN variants for computer vision: History, architecture, application, challenges and future scope. Electronics, 10(20), 2470. https://doi.org/10.3390/electronics10202470

Dif, N., Attaoui, M. O., Elberrichi, Z., Lebbah, M., & Azzag, H. (2021). Transfer learning from synthetic labels for histopathological images classification. Applied Intelligence, 52(1), 358–377. https://doi.org/10.1007/s10489-021-02425-z

Dong, M., Cioffi, G., Wang, J., Waite, K. A., Ostrom, Q. T., Kruchko, C., Lathia, J. D., Rubin, J. B., Berens, M. E., Connor, J., & Barnholtz-Sloan, J. S. (2020). Sex differences in cancer incidence and survival: A pan-cancer analysis. Cancer Epidemiology Biomarkers & Prevention, 29(7), 1389–1397. https://doi.org/10.1158/1055-9965.epi-20-0036

Elazab, N., Soliman, H., El-Sappagh, S., Islam, S. M. R., & Elmogy, M. (2020). Objective diagnosis for histopathological images based on machine learning techniques: Classical approaches and new trends. Mathematics, 8(11), 1863. https://doi.org/10.3390/math8111863

Ellsworth, R. E., Blackburn, H. L., Shriver, C. D., Soon-Shiong, P., & Ellsworth, D. L. (2017). Molecular heterogeneity in breast cancer: State of the science and implications for patient care. Seminars in Cell & Developmental Biology, 64, 65–72. https://doi.org/10.1016/j.semcdb.2016.08.025

Elmore, J. G., Longton, G. M., Carney, P. A., Geller, B. M., Onega, T., Tosteson, A. N. A., Nelson, H. D., Pepe, M. S., Allison, K. H., Schnitt, S. J., O'Malley, F. P., & Weaver, D. L. (2015). Diagnostic concordance among pathologists interpreting breast biopsy specimens. JAMA, 313(11), 1122–1132. https://doi.org/10.1001/jama.2015.1405

ELSTON, C. W., & ELLIS, I. O. (1991). Pathological prognostic factors in breast cancer. I. the value of histological grade in breast cancer: Experience from a large study with long-term follow-up. Histopathology, 19(5), 403–410. https://doi.org/10.1111/j.1365-2559.1991.tb00229.x

Ferlay, J., Colombet, M., Soerjomataram, I., Parkin, D. M., Piñeros, M., Znaor, A., & Bray, F. (2021). Cancer statistics for the year 2020: An overview. International Journal of Cancer, 149(4), 778–789. https://doi.org/10.1002/ijc.33588

Ferreira, C., Melo, T., Sousa, P., Meyer, M., Shakibapour, E., Costa, P., & Aurélio Campilho. (2018). Classification of breast cancer histology images through transfer learning using a pretrained inception resnet V2. International Conference Image Analysis and Recognition, 763–770. https://doi.org/10.1007/978-3-319-93000-8_86

George, Y. M., Zayed, H. H., Roushdy, M. I., & Elbagoury, B. M. (2014). Remote computer-aided breast cancer detection and diagnosis system based on cytological images. IEEE Systems Journal, 8(3), 949–964. https://doi.org/10.1109/jsyst.2013.2279415

Hameed, Z., Zahia, S., Garcia-Zapirain, B., Javier Aguirre, J., & María Vanegas, A. (2020). Breast cancer histopathology image classification using an ensemble of deep learning models. Sensors, 20(16), 4373. https://doi.org/10.3390/s20164373

Juppet, Q., De Martino, F., Marcandalli, E., Weigert, M., Burri, O., Unser, M., Brisken, C., & Sage, D. (2021). Deep learning enables individual xenograft cell classification in histological images by analysis of contextual features. Journal of Mammary Gland Biology and Neoplasia, 26(2), 101–112. https://doi.org/10.1007/s10911-021-09485-4

Khan, S., Islam, N., Jan, Z., Ud Din, I., & Rodrigues, J. J. P. C. (2019). A novel deep learning based framework for the detection and classification of breast cancer using transfer learning. Pattern Recognition Letters, 125, 1–6. https://doi.org/10.1016/j.patrec.2019.03.022

Kumar, A., Singh, S. K., Saxena, S., Lakshmanan, K., Sangaiah, A. K., Chauhan, H., Shrivastava, S., & Singh, R. K. (2020). Deep feature learning for histopathological image classification of canine mammary tumors and human breast cancer. Information Sciences, 508, 405–421. https://doi.org/10.1016/j.ins.2019.08.072

Liang, Y., Yang, J., Quan, X., & Zhang, H. (2019). Metastatic breast cancer recognition in histopathology images using convolutional neural network with attention mechanism. 2019 Chinese Automation Congress (CAC), 2922–2926. https://doi.org/10.1109/cac48633.2019.8997460

Mani, C., Kamalakannan, N. J., Rangaiah, N. Y. P., & Anand, N. S. (2023). A bio-inspired method for breast histopathology image classification using transfer learning. Journal of Artificial Intelligence and Technology, 4(2). https://doi.org/10.37965/jait.2023.0246

Meng, Z., Zhao, Z., & Su, F. (2019). Multi-classification of breast cancer histology images by using gravitation loss. ICASSP 2022 - 2022 IEEE International Conference on Acoustics, Speech and Signal Processing (ICASSP), 1030–1034. https://doi.org/10.1109/icassp.2019.8683592

Mohammed, H. A., Kareem, S. W., & Mohammed, A. S. (2022). A comparative evaluation of deep learning methods in digital image classification. Kufa Journal of Engineering, 13(4), 53–69. https://doi.org/10.30572/2018/kje/130405

Momenimovahed, Z., & Salehiniya, H. (2019). Epidemiological characteristics of and risk factors for breast cancer in the world. Breast Cancer: Targets and Therapy, Volume 11(11), 151–164. https://doi.org/10.2147/bctt.s176070

Murtaza, G., Shuib, L., Wahid Abdul Wahab, A., Mujtaba, G., Mujtaba, G., Raza, G., & Aniza Azmi, N. (2019). Breast cancer classification using digital biopsy histopathology images through transfer learning. Journal of Physics: Conference Series, 1339(1), 012035. https://doi.org/10.1088/1742-6596/1339/1/012035

Nahid, A.-A., Mehrabi, M. A., & Kong, Y. (2018). Histopathological breast cancer image classification by deep neural network techniques guided by local clustering. BioMed Research International, 2018, 1–20. https://doi.org/10.1155/2018/2362108

Nejad, E. M., Affendey, L. S., Latip, R. B., & Bin Ishak, I. (2017). Classification of histopathology images of breast into benign and malignant using a single-layer convolutional neural network. Proceedings of the International Conference on Imaging, Signal Processing and Communication - ICISPC 2017, 50–53. https://doi.org/10.1145/3132300.3132331

Perez, H., & Tah, J. H. M. (2020). Improving the accuracy of convolutional neural networks by identifying and removing outlier images in datasets using t-SNE. Mathematics, 8(5), 662. https://doi.org/10.3390/math8050662

Place, A. E., Jin Huh, S., & Polyak, K. (2011). The microenvironment in breast cancer progression: Biology and implications for treatment. Breast Cancer Research, 13(6). https://doi.org/10.1186/bcr2912

Rock, C. L., Thomson, C. A., Sullivan, K. R., Howe, C. L., Kushi, L. H., Caan, B. J., Neuhouser, M. L., Bandera, E. V., Wang, Y., Robien, K., Basen-Engquist, K. M., Brown, J. C., Courneya, K. S., Crane, T. E., Garcia, D. O., Grant, B. L., Hamilton, K. K., Hartman, S. J., Kenfield, S. A., & Martinez, M. E. (2022). American cancer society nutrition and physical activity guideline for cancer survivors. CA: A Cancer Journal for Clinicians, 72(3), 230–262. https://doi.org/10.3322/caac.21719

Ruqaya Alaa, Hussein, E., & Hilal Al-libawy. (2024). Object detection algorithms implementation on embedded devices: Challenges and suggested solutions. Kufa Journal of Engineering, 15(3), 148–169. https://doi.org/10.30572/2018/KJE/150309

Shafiq, M., & Gu, Z. (2022). Deep residual learning for image recognition: A survey. Applied Sciences, 12(18), 8972. https://doi.org/10.3390/app12188972

Sivalingan. (2024). Cloud-Smart surveillance: Enhancing anomaly detection in video streams with df-convlstm-based vae-gan. Kufa Journal of Engineering, 15(4), 125–140. https://doi.org/10.30572/2018/kje/150409

Sreelekshmi, V., Pavithran, K., & Nair, J. J. (2024). SwinCNN: An integrated swin trasformer and CNN for improved breast cancer grade classification. IEEE Access, 12, 68697–68710. https://doi.org/10.1109/access.2024.3397667

Toğaçar, M., Özkurt, K. B., Ergen, B., & Cömert, Z. (2020). BreastNet: A novel convolutional neural network model through histopathological images for the diagnosis of breast cancer. Physica A: Statistical Mechanics and Its Applications, 545, 123592. https://doi.org/10.1016/j.physa.2019.123592

Ukwuoma, C. C., Hossain, M. A., Jackson, J. K., Nneji, G. U., Monday, H. N., & Qin, Z. (2022). Multi-Classification of breast cancer lesions in histopathological images using deep_pachi: Multiple self-attention head. Diagnostics, 12(5), 1152. https://doi.org/10.3390/diagnostics12051152

Vallabhajosyula, S., Sistla, V., & Kolli, V. K. K. (2021). Transfer learning-based deep ensemble neural network for plant leaf disease detection. Journal of Plant Diseases and Protection, 129(3). https://doi.org/10.1007/s41348-021-00465-8

Wilkinson, L., & Gathani, T. (2021). Understanding breast cancer as a global health concern. The British Journal of Radiology, 95(1130), 20211033. https://doi.org/10.1259/bjr.20211033

Xie, J., Liu, R., Luttrell, J., & Zhang, C. (2019). Deep learning based analysis of histopathological images of breast cancer. Frontiers in Genetics, 10. https://doi.org/10.3389/fgene.2019.00080

Yan, R., Ren, F., Wang, Z., Wang, L., Zhang, T., Liu, Y., Rao, X., Zheng, C., & Zhang, F. (2019). Breast cancer histopathological image classification using a hybrid deep neural network. Methods, 173, 52–60. https://doi.org/10.1016/j.ymeth.2019.06.014

Yao, H., Zhang, X., Zhou, X., & Liu, S. (2019). Parallel structure deep neural network using CNN and RNN with an attention mechanism for breast cancer histology image classification. Cancers, 11(12), 1901. https://doi.org/10.3390/cancers11121901

Yousef, R., Gupta, G., Yousef, N., & Khari, M. (2022). A holistic overview of deep learning approach in medical imaging. Multimedia Systems, 28(3), 881–914. https://doi.org/10.1007/s00530-021-00884-5

Zakaria, N., & Yana. (2024). A review study of the visual geometry group approaches for image classification. Journal of Applied Science, Technology and Computing, 1(1), 14–28. https://publisher.uthm.edu.my/ojs/index.php/jastec/article/view/16010

Zhou, Y., Zhang, C., & Gao, S. (2022). Breast cancer classification from histopathological images using resolution adaptive network. IEEE Access, 10, 35977–35991. https://doi.org/10.1109/access.2022.3163822

Zhu, C., Song, F., Wang, Y., Dong, H., Guo, Y., & Liu, J. (2019). Breast cancer histopathology image classification through assembling multiple compact cnns. BMC Medical Informatics and Decision Making, 19(1). https://doi.org/10.1186/s12911-019-0913-x.